DOI: 10.17344/acsi.2025.9145 *Acta Chim. Slov.* **2025,** *72,* 154–163

Scientific paper

Upcycling of Plastic Waste Into Multi-Walled Carbon Nanotubes as Efficient Organic Dye Adsorbent

Gordana Bogoeva-Gaceva,[1,2*] Meri Sokolovska,[3] Viktor Stefov,[3,2] Metodija Najdoski[3] and Sebastijan Kovačič[4,5*]

[1] *Faculty of Technology and Metallurgy, Ss. Cyril and Methodius University - Skopje, 1000 Skopje, R.N. Macedonia*

[2] *Research Center for Environment and Materials, Macedonian Academy of Sciences and Arts, Skopje, R.N. Macedonia*

[3] *Institute of Chemistry, Faculty of Natural Sciences and Mathematics, Ss. Cyril and Methodius University, 1000 Skopje, R.N. Macedonia*

[4] *National Institute of Chemistry, Hajdrihova 19, 1001 Ljubljana, Slovenia*

[5] *Catalysis and Organic Synthesis research group, Laboratory for Organic and Polymer Chemistry, Faculty of Chemistry and Chemical Engineering, University of Maribor, Smetanova 17, SI-2000 Maribor, Slovenia*

** Corresponding author: E-mail: gordana@tmf.ukim.edu.mk sebastijan.kovacic@um.si*

Received: 01-08-2025

Abstract

Multi-walled CNTs with an average diameter of about 80 nm, a length of several micrometers and surface area (S_{BET}) of 100 $m^2\ g^{-1}$ were obtained by pyrolysis of low-density polyethylene waste. The potential of the resulting MWCNTs material to purify water containing organic dyes was tested with Bezaktiv Blau HE-RM (BB) and Bezaktiv Rot S-3B (BR) reactive dyes. 200 mg L^{-1} MWCNT material was used to follow the adsorption of 30 mg L^{-1}, 40 mg L^{-1}, 50 mg L^{-1} and 60 mg L^{-1} BB and BR at pH 3 and a temperature of ~25 °C. The results have shown that this material has a high potential as a sorbent, and its adsorption capacity of 257 mg g^{-1} (for Bezaktiv Blau HE-RM) and 213 mg g^{-1} (for Bezaktiv Rot) is close to some commercial MWCNTs and functionalized MWCNT-based adsorbents. The adsorption process was very fast, reaching 80–90% of the dye removal in 10–15 minutes, and the equilibrium time was reached in 40–60 minutes. The adsorption isotherm showed that the Langmuir model was more suitable than the Freundlich model for describing the adsorption properties of the pollutants.

Keywords: Adsorption; anionic dyes; upcycling plastics waste; carbon nanotubes

1. Introduction

Wastewater from the textile industry affects environmental conditions by generating a large amount of colored and toxic outlets. Among them, dyes are considered the main pollutants due to their stability and low biodegradability. Reactive dyes are among widely used dyes in the textile industry, accounting for 29% of all other textile dyes and more than 50% of global consumption of dyes used for cellulosic fibers coloring.[1,2] The wastewater from the dyeing process discharged into a natural aquatic system not only reduces light transmission, but also has a negative effect on the photochemical activity of the water system and can cause mutations in aquatic organisms. It is estimated that 10–15% of the dye is lost in the wastewater during the dyeing process.[3] Dyes are removed from wastewaters by membrane filtration, ion-exchange, chemical oxidation, degradation, flotation, electrochemical treatment and adsorption.

In wastewater remediation, adsorption over highly porous materials has attracted a lot of attention due to its high efficiency, low energy consumption and simple design.[4] Various synthetic ingredients have been effectively used as adsorbents to remove contaminants from water,[5–8] including engineered nanomaterials.[9] The most commonly used adsorbent is activated carbon, which is produced from various waste materials and is distinguished by large

surface area, good adsorption capacity and the ability to modify/tune its external chemical functional groups and structural properties.[10] Recently, the use of carbon nanotubes (CNTs), especially multi-walled CNTs (MWCNTs), for adsorption applications has gained interest.[11,12] Their large specific surface area, small pore size and hollow structural characteristics proven that MWCNTs have great potential for the adsorption of many types of organic and inorganic pollutants from the aqueous streams.[13–16] In terms of environmental responsibility and cost efficiency, the production of CNT adsorbents is equally important. Common methods for synthesizing CNTs are chemical vapor deposition (CVD), arc discharge and laser ablation.[17] Recently, however, several studies have reported on the conversion of plastic waste into CNTs with high application value. One such approach to managing plastic waste is upcycling, a technology that uses pyrolysis to convert raw materials into value-added products.[18,19]

In our previous study, the adsorption potential of MWCNTs obtained by pyrolysis of waste plastics was assessed by evaluating its adsorption capacity for reactive textile dye, Bezaktiv Blau HE-RM.[20] The adsorption of dyes by various carbonaceous materials has been reported in numerous studies. The dye adsorption capacities of untreated CNTs are quite low but can be significantly improved by functionalization/modification.[9,21] Functionalization increases the number of oxygen, nitrogen or other groups on the surface of the CNTs and improves their dispersibility and thus the specific surface area.[22] The removal capacity of Methylene blue by amorphous carbon was 194 mg g^{-1}, while it reaches 350 mg g^{-1} for activated carbon.[9] The adsorption capacity of activated carbon prepared from prickly pear cake activation with phosphoric acid for Methyl orange dye was 336 mg g^{-1} at temperature 20 °C and pH ~7. This value was much higher than that of the activated CNTs (149 mg g^{-1}) for the same dye. The equilibrium adsorption data were best described by the Freundlich model.[23] The adsorption capacities of nano-Fe_3O_4, graphene oxide, CNT-chitosan and other composite nanomaterials are discussed in the work of Salamatinia.[24] Interestingly, the adsorption capacity of graphene oxide for Methylene blue (81.97 mg g^{-1}) was much lower compared to CNTs with chitosan support. Depending on the surface area of the CNTs and the molecular structure of the cationic and anionic dyes (planar or non-planar), their adsorption capacity can be between 27.6 and 152 mg g^{-1}. Using the Langmuir adsorption model, values for q_{max} of ~100 to ~500 mg g^{-1} were found for MWCNTs doses 250–50 mg L^{-1} for Methyl violet dye.[25] A comparison of the adsorption capacities of different adsorbents for the anionic dyes methyl orange, Congo red, Reactive blue 4, Reactive red M-2BE, Direct red and Acid Blue [26] has shown that the modification of MWCNTs was a promising way to drastically improve the dye removal rate (from less than 100 mg g^{-1} to ~1000 mg g^{-1}). Functionalization of inorganic adsorbent for anionic dyes by acidic treatment was applied to influence the electrostatic attraction between the clay surface and the dye molecule, resulting in an improvement of the adsorption capacity from 2.2 mg g^{-1} to 67.4 mg g^{-1}.[8] A recently published review provides an overview of reactive dye-containing wastewater treatment methods, with hybrid technologies as a promising solution to achieve higher efficiency and effectiveness.[27]

In addition to adsorption capacity, however, kinetics is also one of the fundamental characteristics for evaluating the adsorption performance of porous adsorbents. Since the adsorption of pollutants on porous adsorbents in batch experiments can be described by a series of successive processes, such as the mass transport of pollutants (adsorbate) in the bulk solution, the diffusion of pollutants through the liquid to the adsorbent surface or the adsorbate diffusion within the adsorbent's porous structure, an understanding of the adsorption kinetics is a basic prerequisite for the optimal design of adsorbents and adsorption processes.[28,29] Therefore, the aim of this work is to investigate both kinetic and equilibrium adsorption of two reactive dyes onto MWCNTs carbonaceous material as an adsorbent.

2. Experimental

2. 1. Materials

MWCNT material was obtained from low-density polyethylene waste by pyrolytic degradation using analytical grade cobalt(II) acetate dihydrate (Merck, Germany), as a catalyst in a simple one-stage procedure, as described in detail in our earlier publication.[30] Carbonaceous MWCNT material (CM) was employed in adsorption experiments without any further modification/treatment. Bezaktive Blau HE-RM (BB) and Bezaktive Rot S-3B (BR) reactive (anionic) dyes were supplied by CHT/Bezema. Hydrochloric acid (analytical grade, Merck, Germany), was used for pH dye solution adjustment.

2. 2. Characterization of MWCNT

Scanning electron microscopy (SEM) was performed on Thermo Fisher Verios 4G HP scanning electron microscope. The presence of cobalt particles was additionally characterized using STEM-in-SEM imaging in high-angle annular dark-field (HAADF) and bright-field (BF) modes as well as an energy-dispersive X-ray (EDX) analysis. For both analyses, the solid MWCNT samples were first diluted in absolute ethanol, sonicated for a few seconds to disperse them and then dropped onto the carbon support grids and dried. Nitrogen physisorption analysis was determined from the adsorption and desorption isotherms of N_2 at –196 °C using a TriStar II 3020 instrument (Micromeritics Instrument, Norcross, GA, USA). The specific surface area of the samples was calculated by applying the B.E.T. theory to the nitrogen adsorption data within the

0.06–0.30 P/P_0 range. The MWCNT densities (ρ_P) (an average of 10 consecutive measurements) were evaluated using a fully automated, highly precision helium pycnometry (Ultrapyc 5000 by Anton Paar).

2. 3. Adsorption Experiments

The dye absorbance was measured at 570 nm wavelength for BB and 540 nm wavelength for BR, using a Cary 50 model Varian UV-Vis Spectrophotometer. The calibration curve of BB and BR are shown in Figure 1. The aqueous solution of dye for adsorption experiments was prepared by diluting stock solution prepared from 1 g of dye powder in 1000 mL deionized water in a volumetric flask, and then the solution was diluted to the desired initial dye mass concentration of 30 mg L^{-1}, 40 mg L^{-1}, 50 mg L^{-1} and 60 mg L^{-1}. An amount of 5–25 mg of carbonaceous adsorbent material (CM) was added to a 100-mL laboratory beaker with 50 mL of dye solution (adjusted to pH = 3), and the beaker was placed on a magnetic stirrer with a stirring bar and stirred for 30 min. The adsorption testing was done at constant temperature of 25 °C. The samples of the solution were taken at predetermined time intervals to measure the dye concentration after contact with the adsorbent. The removal efficiency, *R* (%), was calculated from the final (C_f) and initial (C_o) mass concentrations of the dye in solution:

$$R = \frac{C_o - C_f}{C_o} \cdot 100$$

The adsorption capacity (amount of dye adsorbed onto carbonaceous material, *A*, mg g^{-1}) was calculated by the mass balance relationship:

$$A = \frac{C_o - C_f}{m} \cdot$$

where C_o is the initial dye solution mass concentration in mg L^{-1}, C_f is the final dye solution mass concentration in mg/L^{-1}, *m* is the mass of adsorbent in g, and *V* is the volume of dye solution in L.

3. Results and Discussion

3. 1. Adsorbent (MWCNTs) Properties

The pyrolysis of low-density polyethylene waste was carried out in a simple one-step process in the presence of cobalt(II) acetate dihydrate (CoAc) as a catalyst, where MWCNTs begin to form around the cobalt nanocatalyst obtained from the dissociation of CoAc. First, STEM-in-SEM imaging was performed to investigate the morphological properties of the produced carbon material. As depicted in Figure 2, after heating low-density polyethylene waste at 700 °C for three hours, MWCNTs with an average diameter of about 80 nm and a length of several micrometers were formed, with the supported Co-nanocatalyst at the end of each nanotube. To confirm the presence of Co particles, we performed additional characterization using high-angle annular dark-field (HAADF) and bright-field (BF) modes in STEM mode. Atomic-resolution Z-contrast HAADF- and BF-STEM images of Co/MWCNT are shown in Figure 2b and 2c and revealed Co atoms at the end of the MWCNT. Furthermore, EDXS mapping of the selected cross-section of the MWCNTs confirmed that the nanotubes indeed contain nano-sized Co particles.

The porous properties and the associated specific surface area were further analyzed by nitrogen adsorption–desorption measurements. The shape of the isotherms is reminiscent of that of microporous materials following the type I isotherm, with a clear increase in N_2 uptake in the P/P_0 range up to 0.1 and a well-defined hysteresis loop indicating the presence of a certain volume of mesopores. The meso-microporous structure is reflected in an S_{BET} of about 100 m^2 g^{-1} (Figure 3). Next, the skeletal (true) density was determined by helium pycnometry and

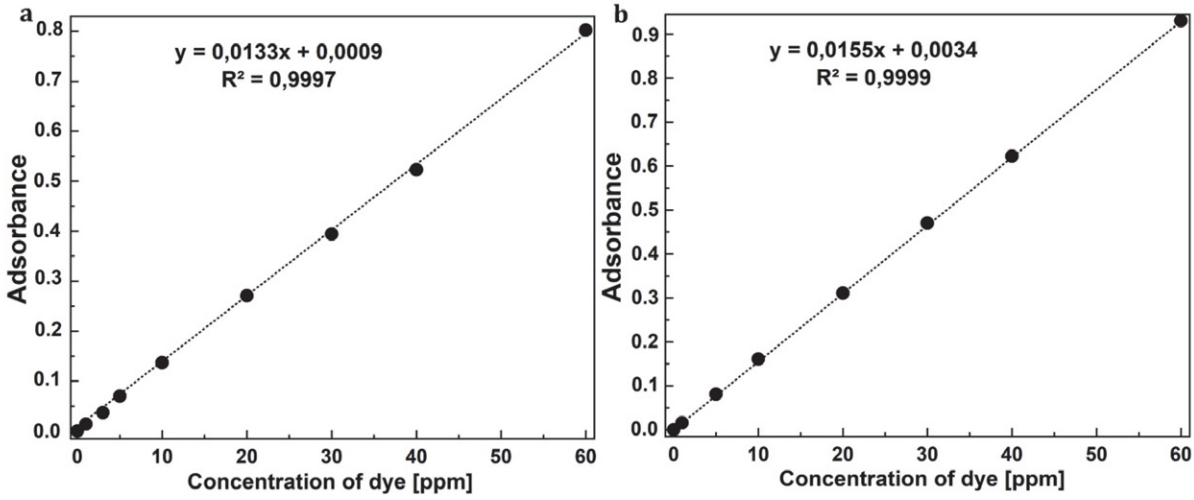

Figure 1. Calibration curve of Bezaktiv Blau HE-RM (a) and Bezaktiv Rot S-3B (b) reactive dyes.

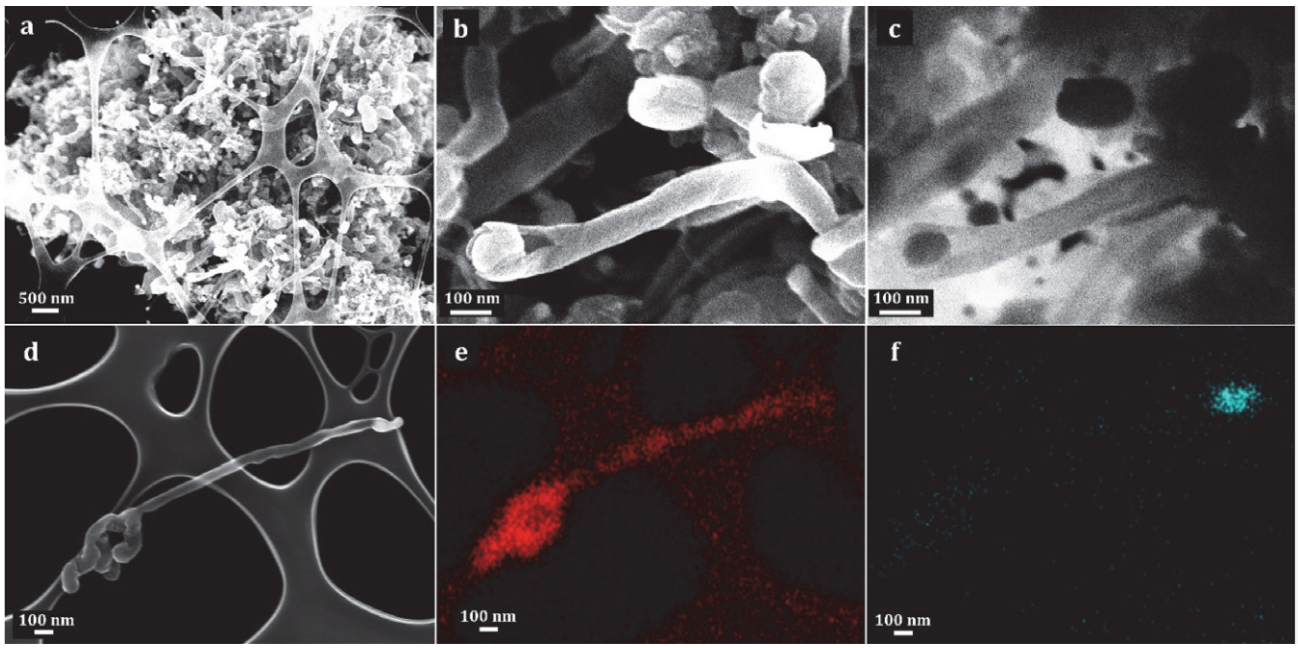

Figure 2. STEM micrographs (a, d), STEM in HAADF mode (b), STEM in BF mode (c) and EDXS elemental mapping for the carbon (e) and cobalt (f) of the Co/MWCNT.

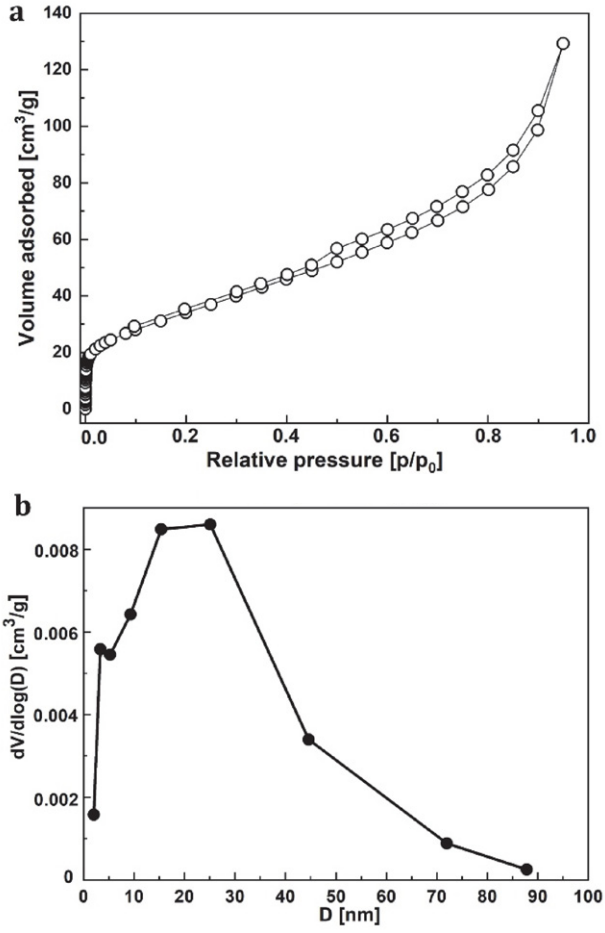

Figure 3. N_2 isotherm of the Co/MWCNT (A) and the pores size distribution plot (B).

found to be 2.5516 g cm^{-3}, which is slightly higher than expected for MWCNTs (2.100 g cm^{-3}), indicating that the MWCNTs are tipped with nanosized metallic Co as also shown in Figure 2.

The use of waste-derived carbonaceous materials holds great potential as a cost-effective adsorbent for organic dye removal, especially those with large surface areas. Next, the potential of the as obtained MWCNT to purify water containing reactive dyes was tested using Bezaktiv Blau HE-RM and Bezaktiv Rot S-3B reactive dyes.

3. 2. The effect of Various Parameters on Dye Adsorption

The adsorption process depends primarily on the contact area between the solid adsorbent and the dye molecule, and the dispersion of the CM is an important factor in the efficiency of dye removal. Under the experimental conditions used, the dispersibility of the MWCNTs was sufficient so that it was not necessary to modify its surface chemistry. The MWCNTs contains cobalt (originating from the catalyst), which can dissolve in solution under acidic conditions. To verify the presence of cobalt in the UV-spectra of the two dyes, an experiment was performed with cobalt-containing dye solution at pH = 3. The results showed that the difference in the spectra of dye solutions with and without cobalt was negligible. The main mechanism of dye adsorption by carbon nanotubes depends on the nature of the dyes – anionic or cationic – and on the surface chemistry of the adsorbent. However, in most cases, it is difficult to predict the mechanism of adsorption, and different possible interactions between CNTs and dyes

have been proposed.[31] Hydrophobic, van der Waals forces, π-π stacking, hydrogen bonding, and electrostatic interactions can act simultaneously or individually.[32] Several main factors play a role in dye adsorption on CNTs, such as the initial mass concentration of the dye, the pH of the solution, the dosage of the adsorbent, and the temperature. Experiments by Liu[33] have shown that the driving force of interaction between CNTs and dyes is the molecular structure of the dye, which is strongly influenced by the π-π bonds, as well as the charge of the CNTs and the dyes.[34] In general, CNTs are positively charged in a wide pH range between 10 and 30 mV, as shown by measurements of the zeta potential.[35] Therefore, CNTs are expected to be more favorable for the adsorption of anionic azo dyes than for cationic dyes, although the conformational structure of a dye also plays an important role.

Effect of initial pH values. The pH of the solution is an important factor that influences the process of dye adsorption by CNTs, through controlling the strength of electrostatic charges in the solution or ionized dye particles. Figure 4 (a, b) shows the variation of dye adsorption on MWCNTs of BB and BR dyes at different pH values. As can be seen from Figure 4 the acidic conditions were favorable for the adsorption of both dyes on MWCNTs.

The results are consistent with the findings of Moradi,[26] who showed that a low pH of the solution was preferred for the adsorption of reactive dyes on CNTs, but also on activated carbon.[36] All further experiments were carried out at pH = 3.

Effect of dosage of MWCNTs. The effect of MWCNT dosage on dye removal is shown in Figure 4 (c, d), where we can observe that increasing the amount of adsorbent (in the range of 400–500 mg L^{-1}) increases the efficiency of dye removal. The percentage of dye removal from the solution increases from 40% (at a MWCNTs dose of 5 mg (100 mg L^{-1})) to 98.6–99.5% (at the CM dose of 20 – 25 mg (400–500 mg L^{-1})) for BB, and from 38% to 98–99% for BR (at the above mention MWCNTs doses), which is due to the larger MWCNT surface area and more available adsorbent sites.

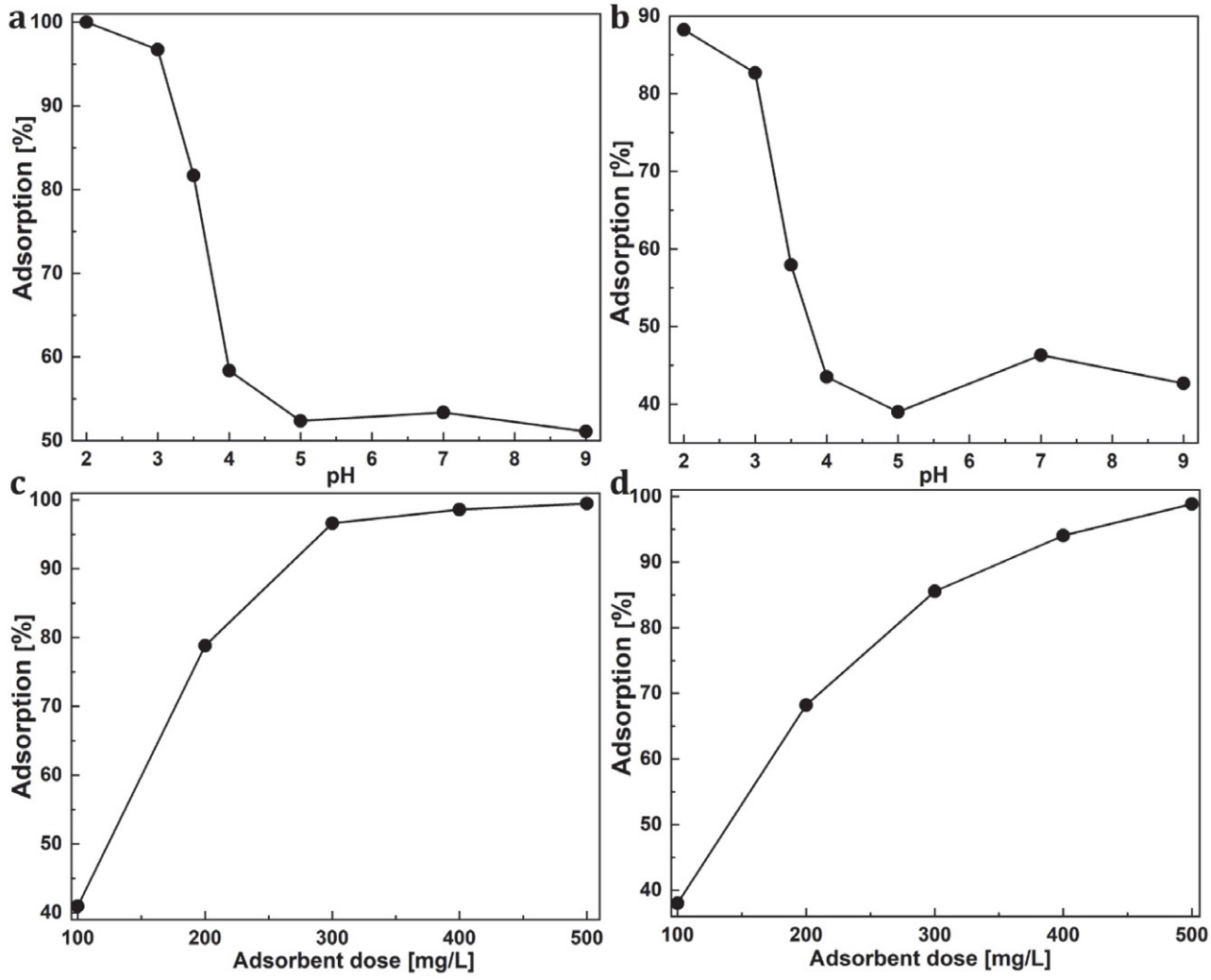

Figure 4. Effect of solution pH on dyes removal rate: for BB (a) and for BR (b) (the contact time for both dyes was ~35 min) and effect of MWCNTs dosage on BB dye adsorption (c) and BR dye adsorption (d) (contact time = 30 min; pH = 3; C_0 = 50 mg L^{-1}).

Table 1. The effect of adsorbent dose on its adsorption capacity for BB and BR dyes (pH = 3; t = 30 min)

BB		BR	
Adsorbent dose / mg L^{-1}	Adsorption capacity / mg g^{-1}	Adsorbent dose / mg L^{-1}	Adsorption capacity / mg g^{-1}
100	245.79	100	228.00
200	236.43	200	204.64
300	193.21	300	171.05
400	147.91	400	141.03
500	119.38	500	118.63

The effect of MWCNTs dose on adsorption capacity is analyzed for the initial dye concentration of 50 mg L^{-1} and the results are also shown in Table 1 for both dyes. The dye removal efficiency for both reactive dyes increased by increasing doses of MWCNTs adsorbent. The highest values of adsorption capacity determined for the dyes BB and BR were 246 mg g^{-1} and 228 mg g^{-1}, respectively.

Effect of initial dye concentration. The effect of the initial dye concentration in the solution (30–60 mg L^{-1}) on the efficiency of its removal is shown in Figure 5. It is obvious that the removal efficiency of the dye decreased with increasing dye concentration, as fewer surface-active sites were available at constant adsorbent dosage. In addition, the mass transfer resistance inhibited the adsorption of dye molecules from the solution phase to the surface of the MWCNTs. The process is faster for BB dye, and the time of 40 to 50 minutes is sufficient to reach equilibrium dye adsorption (dye removal of 99% at the lower initial BB concentrations of 30 mg L^{-1} and 40 mg L^{-1}). The results for BB also show that adsorption is initially very fast, reaching more than 87–96% in the first 10 minutes of contact time, and then proceeding slowly to reaction equilibrium. The process for BR is also very fast in the first minutes, reaching over 75–88% adsorption in 10 minutes, and then the further adsorption of the dye is slowed down (80–88% adsorp-

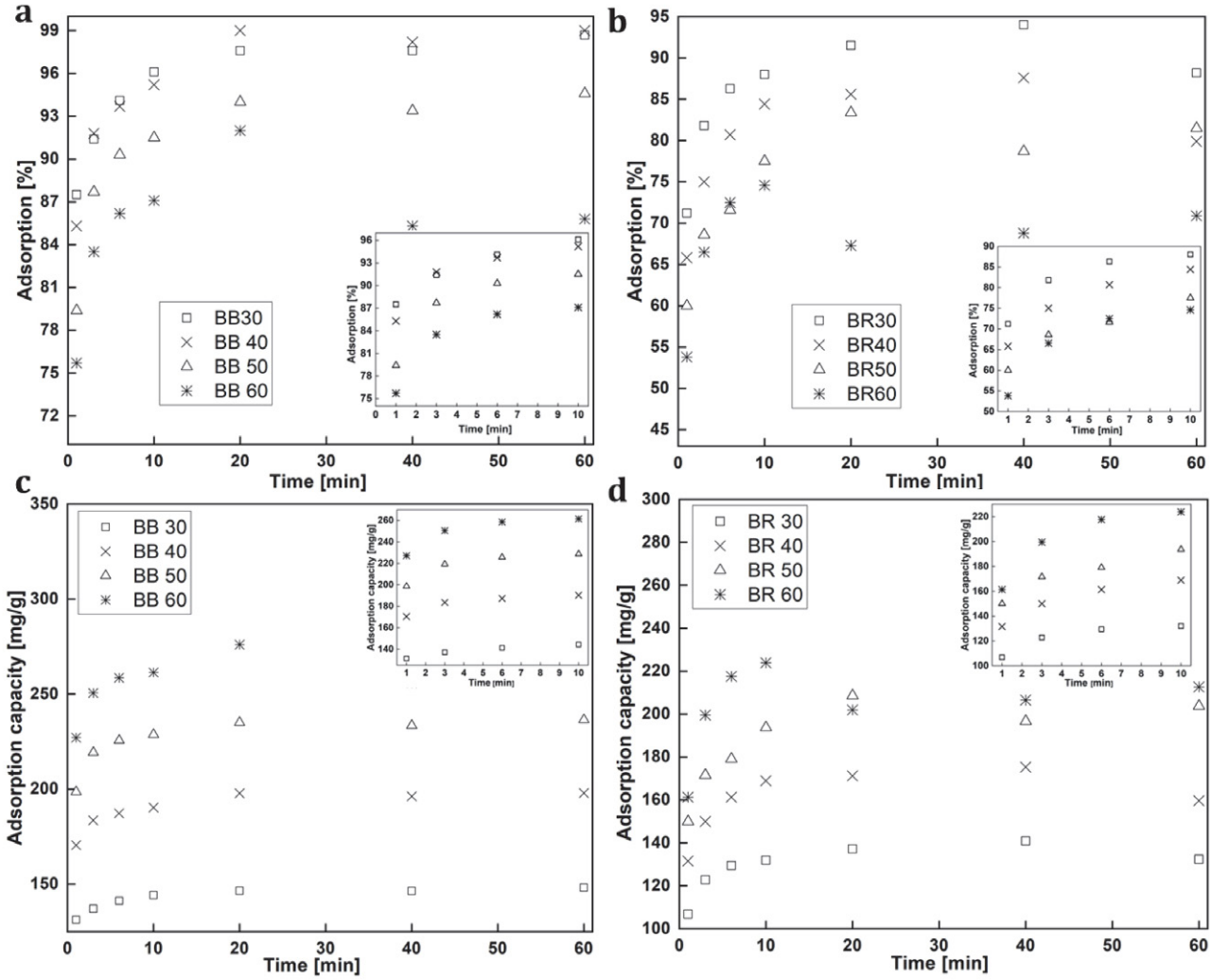

Figure 5. Effect of contact time on BB (A, C) and BR (B, D) adsorption by MWCNTs (pH = 3; MWCNTs dose = 200 mg L^{-1}; C_o = 30 mg L^{-1}, 40 mg L^{-1}, 50 mg L^{-1} and 60 mg L^{-1}).

tion is reached after 60 minutes). The results show that the spaces available for adsorption are mainly located on the outer surface of the MWCNTs, and that adsorption is less dependent on the meso-microporous structure. This is in contrast to the mechanism of adsorption on activated carbon, which mainly depends on its porous structure, and it takes time for the adsorbents to diffuse through the pores.[37]

For both reactive dyes, the maximum adsorption capacity was 148 mg g^{-1} (BB) and 132 mg g^{-1} (BR) under the investigated test conditions with a low adsorbent dosage and an initial dye concentration of 30 mg L^{-1} (Figure 6). The initial dye concentration has a major impact on dye removal efficiency as it depends on the direct relationship between the amount of dye and the sites available for adsorption on the MWCNTs. As the initial concentration of the dye increases, the adsorption capacity changes as follows: 198 mg g^{-1} (C_o = 40 mg L^{-1}), 236 mg g^{-1} (C_o = 50 mg L^{-1}), 257 mg g^{-1} (C_o = 60 mg L^{-1}) for BB; and 160 mg g^{-1} (C_o = 40 mg L^{-1}), 204 mg g^{-1} (C_o = 50 mg L^{-1}), 213 mg g^{-1} (C_o = 60 mg L^{-1}) for BR.

3. 3. Adsorption Isotherms

For further analysis of the adsorption process, the Langmuir and Freundlich isotherm models were used to fit the experimental data. The Langmuir isotherm is applied to homogeneous adsorption under the following assumptions: (a) all adsorption sites are identical; (b) each site retains one molecule of the given compound; and (c) all sites are energetically and sterically independent of the amount adsorbed. The Freundlich isotherm model, on the other hand, assumes sorption on a heterogeneous surface on which there are many different types of available sites with different free sorption energies that are not limited by the formation of a monolayer. Therefore, in this study, the adsorption isotherm models of Langmuir[38] and Freundlich[23] are used to describe the relationship between the adsorbate (BB and BR dyes) and the adsorbent (MWCNT). The adsorption of the dye and q_e (mg g^{-1}) at equilibrium was related to the dye equilibrium concentration C_e (mg L^{-1}) by Eqs. (1) and (2).

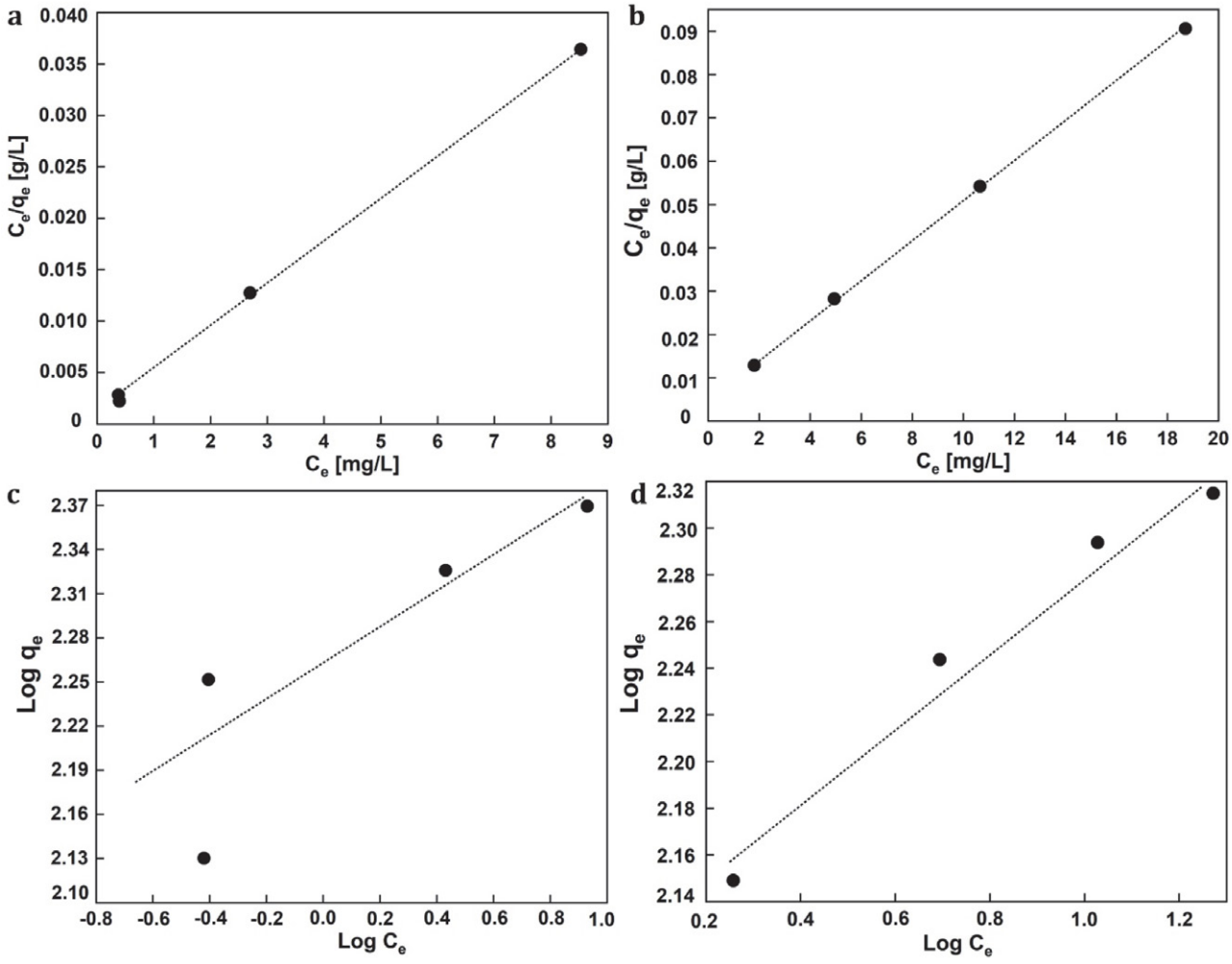

Figure 6. Langmuir isotherms of BB dye (a) and BR dye (b) adsorption and Freundlich isotherms of BB dye (c), and BR dye (d) adsorption on MWCNT (at pH = 3, MWCNT = 200 mg L^{-1}, contact time = 30 min).

The Langmuir isotherm model:

$$C_e/q_e = 1/K_L q_m + (C_e/q_m) \quad (1)$$

C_e (g L^{-1}) is the equilibrium concentration of the dye in the solution, q_e (g g^{-1}) is the amount of dye adsorbed per unit mass of adsorbent, q_m (g g^{-1}) is a constant related to the adsorption capacity (theoretical saturation capacity of the monolayer), and K_L (L g^{-1}) is a constant related to the adsorption rate. q_m is calculated from the slope of the straight line when C_e/q_e is plotted against C_e.

The linear form of the Freundlich isotherm model is represented as follows:

$$\log q_e = \log K_F + (1/n_F)\log C_e \quad (2)$$

K_F (g g^{-1}) (L $g^{-1})^{1/n_F}$ is the constant related to adsorption capacity, and n_F is the adsorption isotherm constant. K_F and $1/n_F$ are calculated from the intercept and slope of the straight line of the plot $\log q_e$ versus $\log C_e$, respectively. The adsorption intensity n_F is used to describe the heterogeneity of the adsorption surface. Values for n_F between 1 and 10 have been shown to indicate a good adsorption potential of the adsorbent.[39] The value $1/n_F$ can vary between 0 and 1. It describes a measure of the heterogeneity of the surface and the adsorption intensity. $1/n_F = 0$ means irreversible adsorption, $0 < 1/n_F < 1$ is a favorable one, and $1/n_F > 1$ means an unfavorable type of isotherm.[40] Figure 6a shows the Langmuir isotherm of the adsorption of BB on MWCNTs. The linear correlation coefficient (R^2) indicates the accuracy of the model and is above 0.9990. The value of q_m obtained is 240.28 mg g^{-1} and the Langmuir constant, K_L = 3.91 L mg^{-1} (see Table 2). The dimensionless equilibrium separation parameter R_L can be calculated from the K_L constant and the initial concentration of the dye solution C_o (mg L^{-1}):

$$R_L = 1/(1 + K_L C_o)$$

If $R_L = 0$, the adsorption is irreversible. When $R < 1$, the adsorption is favorable, $R_L = 1$ suggests a linear, while $R_L > 1$ indicates an unfavorable adsorption of tested dye on the selected substrate.[39,41] The R_L value of BB adsorption on CM was in the range far below 1 (0.0084–0.0042, for the initial dye concentration of C_o 30 mg L^{-1} to 60 mg L^{-1}), testifying that the adsorption process was favorable. The values of R^2 obtained from the linear graph $\log q_e$ versus $\log C_e$ for the Freundlich isotherm (Figure 6c) was 0.7729 and is far below the value obtained for the Langmuir isotherm model (Table 2). The calculated correlation coefficient (R^2) for the Freundlich isotherm (Table 2) shows that the equilibrium data for all tested adsorbent dosages are in better agreement with the Langmuir isotherm than with the Freundlich isotherm, indicating preferential monolayer adsorption. This can be attributed to the size of the BB reactive dye molecules, which are among the smallest textile reactive dyes. As already mentioned, K_F, n_F, and $1/n_F$ are constants related to the Freundlich isotherm, and the determined value of K_F is 178.08 and n_F = 7.21 ($1/n_F$ = 0.1386). The n_F value indicates the degree of nonlinearity between the concentration of the solution and adsorbent. At a value of $n_F = 1$, the adsorption is linear, while $n_F < 1$ indicates that the adsorption process is preferably chemical. However, if the coefficient n_F is greater than 1, then the adsorption is favorable (the physical adsorption is satisfactory),[42] as is determined by Langmuir equilibrium separation parameter, R_L.

A high linear correlation coefficient (R^2 = 0.9998) was also found for the Langmuir isotherm model for the adsorption of BR dye on CM (Figure 6b), with the Langmuir constant K_L = 0.91 L mg^{-1} and q_{max} = 218.12 mg g^{-1} (see Table 2). The values of the Langmuir equilibrium separation parameter, R_L were less than 1, ranging from 0.0355 to 0.0181 for the initial dye concentration of 30 mg L^{-1} and 60 mg L^{-1}. The values of Langmuir and Freundlich isotherm constants determined by the linear fit of Eqs. (1) and (2) are also included in Table 2. The Langmuir isotherm model fits better than the Freundlich isotherm (Figure 6d). The Langmuir isotherm of both dyes on the tested MWCNT was found to be linear over the entire concentration range. The determination coefficients R^2 were extremely high (0.9994). These high degrees of correlation for the Langmuir relationship indicate that a single surface reaction with constant activation energy is the predominant sorption step and possibly the predominant rate-controlling step.

In addition, a high K_L value for BB indicates its strong affinity to MWCNTs, compared to BR dye. Howev-

Table 2. Langmuir and Freundlich isotherm parameters determined for BB and BR dyes.

Adsorption isotherm	Parametars	BB	BR
Langmuir	q_m/mg g^{-1}	240.28	218.12
	K_L/L g^{-1}	3.91	0.91
	R_L (30 mg L^{-1} to 60 mg L^{-1})	(0.0084; 0.0063; 0.0051; 0.0042)	(0.0355; 0.0269; 0.0216; 0.0181)
	R^2	0.9994	0.9998
Freundlich	K_F (mg g^{-1}) (mg L^{-1})	178.08	130.51
	n_F	7.21	6.03
	R^2	0.7729	0.9723

er, both the investigated dyes have the $1/n$ value of less than 1, i.e. 0.1386 for BB and 0.1658 for BR, indicating their favorable adsorption on MWCNTs. The results of our analysis suggest the perspective of upcycling of plastics waste by simple process of pyrolysis for obtaining efficient cost-effective adsorbent for removal of reactive dyes from wastewater effluents.

4. Conclusion

In summary, we have shown that the meso-microporous MWCNTs material with a surface area of about 100 $m^2\ g^{-1}$, obtained in a simple process of pyrolysis of plastic waste, has a high potential as a sorbent for reactive dyes from wastewater effluents. Its adsorption capacity (213–257 mg g^{-1}) for reactive dyes without further modification of its surface is similar to that of some commercial MWCNTs- and functionalized MWCNTs-based adsorbents. The equilibrium adsorption data for the two reactive dyes analyzed, Bezaktiv Blau HE-RMand Bezaktiv Rot S-3B, were best described by the Langmuir model. The conversion of plastic waste into MWCNT material is therefore a practical solution for waste management and at the same time represents a promising contribution to the circular economy.

Acknowledgements

This work was supported by the Ministry of Education, Science and Sport of the Republic of Slovenia and the Slovenian Research and Innovation Agency (Grant P2-0150).

Author contributions

G. B.-G. and M. S. designed and performed the experiments. G. B.-G., M. S., V. S., M. N. and S. K. performed the studies and data analysis. G. B.-G. and M. N. supervised the research. All authors contributed to the writing and editing of the manuscript.

Conflicts of interest

The authors declare no conflicts of interest.

5. References

1. N. R. Jesudoss Hynes, J. Senthil Kumar, H. Kamyab, J. A. Jeniffa Sujana, O. A. Al-Khashman, Y. Kuslu, A. Ene, B. Suresh Kumar, *J. Clean. Prod.* **2020**, *272*, 122636. **DOI:**10.1016/j.jclepro.2020.122636
2. M. Božič, V. Kokol, *Dyes Pigm.* **2008**, *76*, 299–309. **DOI:**10.1016/j.dyepig.2006.05.041
3. R. Kant, *J. Water Resource Prot.* **2012**, *4*, 93–98. **DOI:**10.4236/jwarp.2012.42011
4. N. Hlongwane, P. T. Sekoai, M. Meyyappan, K. Moothi, *Sci. Total Env.* **2019**, *656*, 808–833. **DOI:**10.1016/j.scitotenv.2018.11.257
5. T. Yao, S. Guo, C. Zeng, C. Wang, L. Zhang, *J. Hazard. Mater.* **2015**, *292*, 90–97. **DOI:**10.1016/j.jhazmat.2015.03.014
6. S. Bousba, A. H. Meniai, *Chem. Eng. Trans.* **2013**, *35*, 859–864. **DOI:**10.3303/CET1335143
7. H. Tian, J. Peng, T. Lv, C. Sun, H. He, *J. Solid State Chem.* **2018**, *257*, 40–48. **DOI:**10.1016/j.jssc.2017.09.017
8. J. V. Fernandes, A. M. Rodrigues, R. R. Menezes, G. de A. Neves, *Mater.* **2020** *13*, 3600. **DOI:**10.3390/ma13163600
9. A. S. Adeleye, J. R. Conway, K. Garner, Y. Huang, Y. Su, A. A. Keller, *Chem. Eng. J.* **2016**, *286*, 640–662. **DOI:**10.1016/j.cej.2015.10.105
10. N. U. M. Nizam, M. M. Hanafiah, E. Mahmoudi, A. A Halim, A. W Mohammad. *Sci. Rep.* **2021**, *11*, 8623. **DOI:**10.1038/s41598-021-88084-z
11. V. Gupta, T. Saleh, *Environ. Sci. Pollut. Res.* **2013**, *20*, 2828–2843. **DOI:**10.1007/s11356-013-1524-1
12. R. R. Basca, C. Laurent, A. Peigney, W. S. Basca, T. Vaugien, A. Rousset, *Chem. Phys. Lett.* **2000**, *323*, 566–571. **DOI:**10.1016/S0009-2614(00)00558-3
13. Q. Fang, B. Chen, *Carbon* **2012**, *50*, 2209-2219. **DOI:**10.1016/j.carbon.2012.01.036
14. W. Yan, L. Yan, J. Duan, C. Jing, *J. Hazard. Mater.* **2014**, *273*, 53–60. **DOI:**10.1016/j.jhazmat.2014.03.030
15. Y. Bai, D. Lin, F. Wu, Z. Wang, B. Xing, *Chemosphere* **2010**, *79*, 362–367. **DOI:**10.1016/j.chemosphere.2010.02.023
16. L. Joseph, J. Heo, Y.-G. Park, J. R. V. Flora, Y. Yoon, *Desalination* **2011**, *281*, 68–74. **DOI:**10.1016/j.desal.2011.07.044
17. J. Prasek, J. Drbohlavova, J. Chomoucka, J. Hubalek, O. Jasek, V. Adam, R. Kizek, *J. Mater. Chem.* **2011**, *21*, 15872–15884. **DOI:**10.1039/c1jm12254a
18. D. Yao, H. Yang, Q. Hu, Y. Chen, H. Chen, P. T. Williams, *Appl. Catal. B: Environ.* **2021**, *280*, 119413. **DOI:**10.1016/j.apcatb.2020.119413
19. S. Ha, J. C. Hyun, J. H. Kwak, H. D. Lim, B. S. Youn, S. Cho, H. J. Jin, H. K. Lim, S. M. Lee, Y. S. Yun, *Chem. Eng. J.* **2022**, *437*, 135416. **DOI:**10.1016/j.cej.2022.135416
20. G. Bogoeva-Gaceva, M. Najdoski, V. Stefov, S. Ibishi, *Maced. J. Chem. Chem. Eng.* **2021**, *40*, 321–324. **DOI:**10.20450/mjcce.2021.2424
21. N. Rajesh Jesudoss Hynes, J. Senthil Kumar, Hesam Kamyab, J. Angela Jennifa Sujana, Omar Ali Al-Khashman, Yasemin Kuslu, Antoaneta Ene, B. Suresh Kumar, *J. Clean. Prod.* **2020**, *272*, 122636. **DOI:**10.1016/j.jclepro.2020.122636
22. Y. H. Li, S. Wang, J. Wei, X. Zhang, C. Xu, Z. Luan, D. Wu, B. Wei, *Chem. Phys. Lett.* **2002**, *357*, 263–266. **DOI:**10.1016/S0009-2614(02)00502-X
23. H. Freundlich, *J. Phys. Chem.* **1906**, *57*, 385–470. **DOI:**10.1515/zpch-1907-5723
24. K. B Tan, M. Vakili, B. A. Horri, P. E. Poh, A. Z. Abdullah, B. Salamatinia, *Sep. Purif. Technol.* **2015**, *150*, 229–242. **DOI:**10.1016/j.seppur.2015.07.009
25. M. I. Mohammed, A. A. A. Razak, D. A. H. Al-Timimi, *Adv. Mater. Sci. Eng.* **2014**, *10*, 2014, 3–13.

DOI:10.1155/2014/201052
26. M. Rajabi, K. Mahanpoor, O. Moradi, *RSC Adv.* **2017**, *7*, 47083–47090. **DOI:**10.1039/C7RA09377B
27. S. N. Kamati, J. Yanb, J. Fan, *Water Pract. Technol.* **2024**, *19*, 2712–2733. **DOI:**10.2166/wpt.2024.142
28. S. Jurjevec, E. Žagar, S. Kovačič, *J. Colloid Interface Sci.* **2020**, *575*, 480–488. **DOI:**10.1016/j.jcis.2020.05.016
29. S. Kovačič, N. Drašinac, A. Pintar, E. Žagar, *Langmuir* **2018**, *34*, 10353–10362. **DOI:**10.1021/acs.langmuir.8b01645
30. V. Stefov, M. Najdoski, G. Bogoeva-Gaceva, A. Buzarovska, *Synth. Met.* **2014**, *197*, 159–167. **DOI:**10.1016/j.synthmet.2014.09.011
31. J. G. Yu, X. H Zhao, H. Yang, X. H Chen, Q. Yang, L. Y. Yu, J. H. Jiang, X. Q. Chen, *Sci. Total Environ*. **2014**, *482–483*, 241–251. **DOI:**10.1016/j.scitotenv.2014.02.129
32. M. Rajabi, K. Mahanpoor, O. Moradi, *RSC Adv.* **2017**, *7*, 47083–47090. **DOI:**10.1039/C7RA09377B
33. C. H. Liu, J. J. Li, H. L. Zhang, B. R. Li, Y. Guo, *Colloids Surf. A Physicochem. Eng. Asp.* **2008**, *313–314*, 9–12. **DOI:**10.1016/j.colsurfa.2007.04.062
34. V. K. Gupta, R. Kumar, A. Nayak, T. A. Saleh, M. A. Barakat, *Adv. Colloid Interface Sci.* **2013**, *193–194*, 24–34. **DOI:**10.1016/j.cis.2013.03.003
35. K. Esumi, M. Ishigami, A. Nakajima, K. Sawada, H. Honda, *Carbon* **1996**, *34*, 279–281. **DOI:**10.1016/0008-6223(96)83349-5
36. A. M. Abbas, F. H. Abdulrazzak, W. J. Sabbar, R. A. S. Faraj, *J. Mater. Environ. Sci*. **2020**, *11*, 2007–2015.
37. Y. El maguana, N. Elhadiri, M. Benchanaa, R. Chikri, *J. Chem*. **2020**, *2020*, 1–9. **DOI:**10.1155/2020/2096834
38. I. Langmuir, *J. Am. Chem. Soc*. **1916**, *38*, 2221–2295. **DOI:**10.1021/ja02268a002
39. B. G. Alhogbi, S. Altayeb, E. A. Bahaidarah, M. F. Zawrah, *Processes* **2021**, *9*, 416–436. **DOI:**10.3390/pr9030416
40. M. Kaur, M. Datta, *Sep. Sci. Technol.* **2013**, *48*, 1370–1381. **DOI:**10.1080/01496395.2012.727939
41. Z. Aly, A. Graulet, N. Scales, T. Hanley, *Environ. Sci. Pollut. Res*. **2014**, *21*, 3972–3986. **DOI:**10.1007/s11356-013-2305-6
42. M. Somaia, M. A. Sahar, *Int. J. Ind. Chem.* **2017**, *8*, 121–132. **DOI:**10.1007/s40090-017-0115-2

Povzetek

S pirolizo odpadnega polietilena smo uspešno proizvedli večstenske ogljikove nanocevke (MWCNT) s povprečnim premerom 80 nm, dolžino več mikrometrov in specifično površino (SBET) 100 $m^2\ g^{-1}$. MWCNT smo nato testirali kot adsorbent za odstranjevanje organskih barvil iz vode, pri čemer smo preučevali adsorpcijo dveh reaktivnih barvil: Bezaktiv Blau HE-RM (BB) in Bezaktiv Rot S-3B (BR). Med testiranjem adsorpcije smo proučevali različne koncentracije barvil (30 mg L^{-1}, 40 mg L^{-1}, 50 mg L^{-1} in 60 mg L^{-1}) pri različnih pH vrednostih ter uporabili različne količine MWCNT adsorbenta. Rezultati so pokazali, da ima ta material velik potencial kot adsorbent, saj njegova adsorpcijska kapaciteta znaša 257 mg g^{-1} za Bezaktiv Blau HE-RM in 213 mg g^{-1} za Bezaktiv Rot, kar je primerljivo z nekaterimi komercialnimi adsorbenti. Kinetika adsorpcije je bila izjemna, saj je bilo odstranjenih 80–90% barvila v 10 minutah, ravnotežno stanje pa je bilo doseženo v 40–60 minutah. Za vse proučevane kombinacije smo izračunali tudi Langmuirjevo in Freundlichovo izotermo ter ugotovili, da Langmuirjev model bolje opisuje adsorpcijo MWCNT kot Freundlichov model.